Eur. Phys. J. D **38**, 203–208 (2006)
DOI: 10.1140/epjd/e2006-00020-8

THE EUROPEAN PHYSICAL JOURNAL D

Laser spectroscopy on molecular beam with a time-of-flight mass spectrometer operating in a strong magnetic field

Y. Kimura[a], Y. Kitahama, and K. Takazawa

Tsukuba Magnet Laboratory, National Institute for Materials Science, 3-13 Sakura, Tsukuba, 305-0003 Japan

Received 29 July 2005 / Received in final form 5 January 2006
Published online 31 January 2006 –

Abstract. Experimental set-up for studying effects of a strong magnetic field on a structure and a decay dynamics of molecules, was designed and constructed. A vacuum chamber, in which a molecular beam propagated, was mounted in a bore of a superconducting magnet. Laser light crossed the molecular beam in the magnetic field and excited the molecules. Fragment or parent ions produced through sequential decay processes, were extracted by an electric field parallel to the magnetic field and detected by a microchannel plate. By measuring the time-of-flight from the photo-excitation to the ion-detection, a species of ions — mass and charge state— was identified. A performance of the set-up was demonstrated using the resonance enhanced multiphoton ionization process through the $X^2\Pi - A^2\Sigma^+$ transition of nitric oxide (NO) molecules. A mass resolution $m/\Delta m \geq 180 \pm 6$ was obtained in the field up to 10 T. This was the first successful result demonstrating the sufficient mass resolution obtained by the time-of-flight technique in the strong magnetic field up to 10 T. Parent NO^+ ions were selectively detected by the mass spectrometer and the ion current was measured as a function of the frequency of the laser light. Rotational transition lines were measured with a sufficient S/N ratio in the field up to 10 T.

PACS. 39.10.+j Atomic and molecular beam sources and techniques – 82.80.Rt Time of flight mass spectrometry – 33.55.Be Zeeman and Stark effects

1 Introduction

Effects of a magnetic field on atoms and molecules have been long attractive subjects. In a weak field Zeeman effect was, and in somewhat stronger field Paschen-Back effect was observed. In a stronger field of 2.7 T, quadratic Zeeman effect was observed in highly excited alkali-metal atoms [1]. Highly excited states were selected because they were sensitive to the external field. In a field of 2.5 T, Garton and Tomkins first observed the Landau resonance due to cyclotron motions of electrons induced by the magnetic field, in the continuum above the zero-field ionization limit of Ba atoms [2]. After these earlier studies, a number of studies on the quadratic Zeeman effect of atoms [3–6] and on the Landau resonance of atoms [7–12] were reported. A number of studies were also reviewed in references [13,14].

For molecules, however, since their energy structures are far complicated and the energy of their levels overlaps more complicatedly as the molecular size or the field strength increases, the spectroscopic approaches were difficult. Thus, in most of experiments [15–17] and calculations [18–20] where the effects of the magnetic field were studied, the field strength was limited to low (∼1 T), the species of molecules studied were limited to diatomic or small ones, and only the low energy region below the ionization limit was probed. Takazawa et al. prepared nitric oxide (NO) molecules in gaseous flow in a strong field of 10 T generated by a superconducting magnet, excited them by a double resonance method above the ionization limit and first succeeded in observing Landau levels of molecules. Their success was due to the strong field to extend the energy difference between the neighbouring resonance enough to be resolved and the double resonance technique to reduce the energy-overlapping of the transitions. However, the observed resonance width was broad due to the collision-induced ionization [21]. Therefore, in order to observe the energy structure of highly excited molecules in a magnetic field, they should be prepared under a collision-free condition.

The dissociation is a decay process specific on molecules and important as the most fundamental chemical reactions. Polyatomic molecules have a possibility to dissociate into various species of fragments. The magnetic field would change the branching of the species, because the field effects the dissociation rates through the field-induced coupling interaction [22]. In this way the magnetic

[a] e-mail: kimura.yasuyuki@nims.go.ip

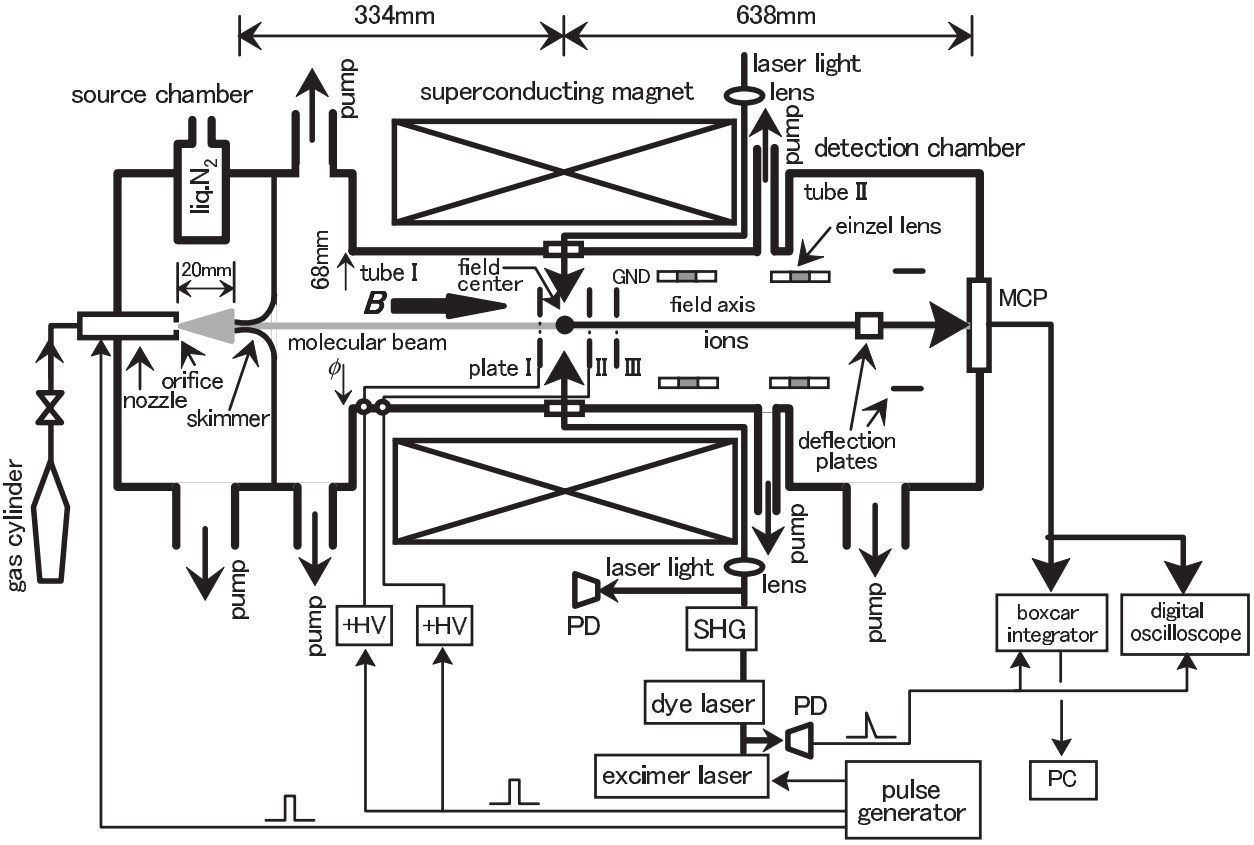

Fig. 1. A schematic view of the experimental set-up.

field can *switch* the dissociation path, and thus can *switch* the chemical reaction. In order to observe such interesting effects, a species identification of the fragments is indispensable not only to identify the dissociation path but also to reduce the energy-overlaping of the exciting transitions.

It is summarized that the effects of the magnetic field on the structure and the dynamics of the molecules are of interest, but a lot of difficulties lie in a experimental research. A newly developed experimental set-up for the laser spectroscopy (double resonance technique) including a superconducting magnet which generates a strong field, a molecular beam source for a collision-free condition, and a mass spectrometer for the species identification, has been designed and constructed. Its performance has been demonstrated using the resonance enhanced multiphoton ionization (REMPI) process on NO molecules.

2 Instrument description

Figure 1 schematically shows the experimental set-up. Magnetic field (0–10 T) was generated by a cryogen-free solenoid-type superconducting magnet cooled by 4 K Gifford-McMahon refrigerator, which had a bore of ϕ 100 mm diameter and 460 mm length (Japan Superconductor Technonogy Inc.). The direction of the magnetic field was coaxial to the axis of the bore ("field axis"). The strength of the field was maximum at 250 mm ("field center") from one of the edges of the bore along the field axis. In a source chamber (250 mm $\times$ 180 mm $\times$ 210 mm) evacuated to 1×10^{-7} Torr, a nozzle with an orifice (ϕ 300 μm) was equipped. The orifice was able to be closed by a piezo element (PI,P-286.23) [23] which could operate without being affected by the magnetic field. Typically, the orifice opened during 180 μs with 10 Hz repetition for gaseous molecules of 3 atm pressure and bunches of molecules were spouted into the chamber through the orifice. A liquid nitrogen trap was equipped for trapping extra molecules effused in the chamber. The pressure in the source chamber was kept $\sim 4 \times 10^{-6}$ Torr during the operation. The molecules were collimated by a conical skimmer (ϕ 700 μm) placed 20 mm downstream from the orifice. The skimmer formed a molecular beam propagating coaxially to the field axis. The molecular beam went into a detection chamber which consisted of two tubes of different diameter. A tube of outer diameter ϕ 82 mm and inner diameter ϕ 68 mm (tube I), was mounted into the bore of the magnet. The pressure in tube I was 1×10^{-6} Torr in operation which was almost same as background pressure.

Laser light was introduced into the detection chamber through a quartz window attached to tube I and focused to the field center by a $f = 400$ mm (focal length) quartz lens. The distance between the field center and the skimmer was 334 mm. At the field center, the light crossed the molecular beam at right angles. If necessary (double

resonance excitation), another laser light propagating antiparallel to the former laser light, was able to be introduced to the field center through another window by the same manner. The laser light excited the molecules in the beam and sequentially parent or fragment ions were produced through their decay process. Three stainless plates (45 mm × 45 mm) with openings (ϕ 30 mm) in their center, covered with high-transmission (>90%) stainless mesh grids, were placed 10 mm upstream (plate I), and 10 mm (plate II), 20 mm (plate III) downstream from the field center along the field axis, respectively. A cw or pulsed high voltages up to 5 kV were supplied to plate I and plate II, independently and plate III was connected to the ground electric potential. Then, double electric field of different strength was generated.

Ions produced at the field center, were accelerated by the electric field and went into another tube (tube II) of inner diameter ϕ 160 mm and length 300 mm, which was connected to tube I at 350 mm downstream from the field center. The pressure in the tube II was 1×10^{-7} Torr in operation, which was almost same as background pressure. The direction of the extraction of the ions was set to be coaxial to the field axis in order to avoid the ions to suffer the Lorentz force. However, a part of the ions traveling off the field axis would be diffused by the Lorentz force. Thus, two sets of einzel lens were equipped to focus them onto the field axis. Two sets of deflection plates were equipped downstream from the einzel lens to bend ions by their electric field. The directions of their electric field were perpendicular to the field axis and orthogonal each other. The ions were finally detected by a microchannel plate (MCP Hamamatsu F4655-11X) attached to a flange at the end of tube II. The distance between the field center and the MCP was 638 mm. The two step acceleration was used to satisfy the Wiley and McLaren condition [24], modified for ions having non-zero initial velocities originated from the translational velocities in the molecular beam.

The electric pulses produced in the MCP following to the incidence of ions, overlapped and made ion current. The ion current was send to a pre-amplifier (Stanford Research System SR445) and then sent to a digital oscilloscope (Tektronix TDS3012) where a time difference from the photo-excitation to the ion detection, i.e. a time-of-flight was measured. The output of the pre-amplifier was also sent to a boxcar integrator (SR250). Its gate-time and gate-width were adjusted by the ion current monitored by the oscilloscope. The integrated voltage was recorded by a personal computer.

3 Instrument performance

For demonstrating a performance, gaseous nitric oxide (NO) molecules of 3 atm pressure was used. An excimer laser light (308 nm, 10 Hz repetition) pumped dye (Coumarin 440) laser light and it was frequency-doubled by a BBO crystal. The UV light (226 nm, band width 0.18 cm^{-1}, ∼0.1 mJ/pulse) linearly polarized perpendicular to the magnetic field was introduced into the field center by the manner described in the previous section. A small portion of the laser light was divided and introduced to a photo-diode detector for monitoring its power.

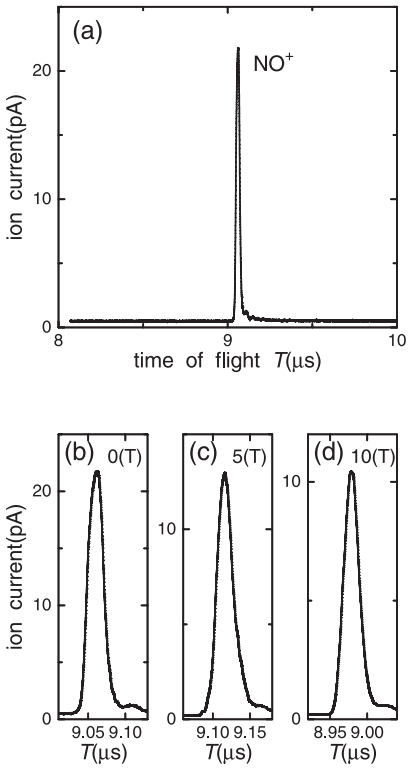

Fig. 2. (a) A typical example of the detected ion current at $B = 0$ T as a function of the time-of-flight T since the photo-excitation (abscissa). The ordinate represents current calculated from the voltage measured by the digital oscilloscope and the gain of both the pre-amplifier and the MCP. The ion current is averaged over 256 scans (laser shots). The transition line excited is marked by an asterisk in Figure 4a. (b) An expanded view of (a) around the peak originated from the NO^+ ions. (c) Similar at $B = 5$ T. (d) Similar at $B = 10$ T.

In a zero magnetic field, the frequency of the laser light was adjusted so that the light excited the NO molecules from the M-degenerated $X^2\Pi_{1/2}(v'' = 0, J'' = 0.5, M \mp 1)$ rotational level to the M-degenerated intermediate $A^2\Sigma^+F_1(v = 0, J = 1.5, M)$ level ($\Delta M = \pm 1$ transition) and further ionized to the NO^+ $X^1\Sigma^+ + e^-$ state through the REMPI process [25], where $v(v'')$ denoted the vibrational quantum number, $J(J'')$ the quantum number associated with the total angular momentum of the NO molecules, M with its projection on the magnetic field direction, respectively. Since this transition had been observed and analyzed in detail in the previous experiment [26], this transition was ideal for demonstrating a performance. A cw voltage of 1.16 kV was supplied to plate I and 0.69 kV to plate II. A typical example of the detected ion current averaged over 256 scans (laser shots), is shown in Figure 2a as a function of the time-of-flight T from the excitation (abscissa). The ordinate represented current calculated from the voltage measured by the digital oscilloscope and the gain of both the pre-amplifier and the MCP. Only a single peak corresponding to the NO^+

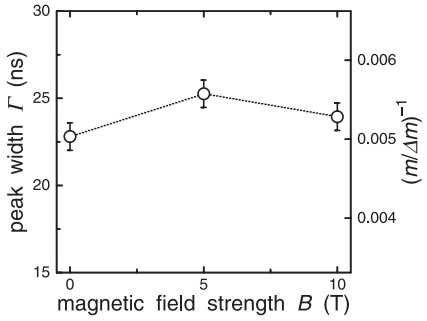

Fig. 3. Variation of the width of the peak Γ originated from the NO^+ ions in the ion current, on the magnetic field strength B. The right ordinate represents the reciprocal of the corresponding mass resolution, $(m/\Delta m)^{-1}$ calculated by the relation $m/\Delta m \simeq T_0/2\Gamma$, where T_0 is assumed to be constant of 9.060 μs.

ions was seen. The peak was fitted by a Gaussian function and its full width at half maximum (line width) Γ was determined to be 23 ns, and the center of the peak T_0 to be 9.060 μs. This procedure was repeated several times. From the averaged values of the obtained Γ and T_0, the mass resolution $m/\Delta m$ was estimated to be 199±7 by the relation $m/\Delta m \simeq T_0/2\Gamma$. The uncertainty was estimated from the standard deviation of the Γ and T_0 measured for several times.

Similar procedures were repeated as the magnetic field strength was increased up to 10 T, as the frequency of the laser light was adjusted so that it was resonant with the transition line whose energy shifted in the field, and as the power of the laser light was adjusted so that the peak was observed with a sufficient S/N ratio. Since the Lorentz force acted on the ions off the field axis was estimated to increase as the field strength increased, it was worried that the trajectory of the ions would be distorted and as the result the width of the peak would increase and the ion current would decrease to the degree that could not be detected. Examples of the peaks in the field of 5 T and 10 T are shown in Figures 2c and 2d. Shapes of the peaks were almost independent of the field strength B. Since the center of the peak T_0 moved around several times of the line width Γ when the voltage supplied to the einzel lens was adjusted, shifts of T_0 in the different field strength seen in Figures 2b–2d had no physical meaning. Averaged values of the width Γ are shown in Figure 3. The width increased slightly as B increased, but corresponding mass resolution $m/\Delta m$ was higher than 180 ± 6 in the range of $B = 0$–10 T, which was sufficient for the species identification. This was the first successful result which demonstrated the sufficient mass resolution obtained by the time-of-flight technique in the strong magnetic field up to 10 T.

A gate-time and a gate-width of the boxcar integrator were fixed to cover the peak originated from the NO^+ ions in the ion current. In a zero field, the frequency of the laser light ν was scanned in the region of the $X^2\Pi_{1/2}(v'' = 0, J+1, M \mp 1) - A^2F_1\Sigma^+(v = 0, J, M)$ transition (P_1-branch), and the integrated ion current $I_0(\nu, B)$ was recorded as a function of ν. Similar procedures were repeated as the field strength was increased up to 10 T. Figure 4a shows the observed ion current $I(\nu, B) = I_0(\nu, B)/W(\nu, B)^2$ normalized by the laser power $W(\nu, B)$.

A population $\sigma_{J''M''}$ of the ground $X^2\Pi_{1/2}(v'' = 0, J''M'')$ sublevel obeyed the Boltzman distribution with a parameter of the rotational temperature T_R [27]. Energy and a wavefunction of the ground $X^2\Pi_{1/2}(v'' = 0, J'', M'')$ sublevel and the intermediate $A^2\Sigma^+F_1(v = 0, J, M)$ sublevel were calculated by diagonalizing their Hamiltonian's including the Zeeman effect. Details of the calculation were described in reference [26]. From the obtained wavefunctions an ionization probability $P(\nu, B)$ by the REMPI process through the $X^2\Pi_{1/2}(v'' = 0, J+1, M \mp 1) - A^2\Sigma^+F_1(v = 0, J, M)$ transition was calculated, on the assumption that the transition probability from the intermediate level to the ionic state was constant against the laser frequency and the transition frequency broaden obeying the Gaussian function of a line width Γ_R. The observed ion current $I(\nu, B)$ should equal to the calculated current defined by the product, $I_{Cal}(\nu, B) = \sigma_{J''M''}P(\nu, B)\gamma(B)$, where $\gamma(B)$ was an efficiency of the detection which was a function of B due to a diffusion of the ions by the Lorenz force. The current $I(\nu, B)$ was fitted to $I_{Cal}(\nu, B)$ with unknown parameters of T_R, Γ_R and $\gamma(B)$. In the fitting procedure, T_R and Γ_R were also treated temporally as a function of B, that made the number of unknown parameters to be 3×11. The obtained T_R and Γ_R had no field dependence. Therefore the rotational temperature T_R was determined to be 27 ± 2 K and the line width Γ_R to be 0.17 ± 0.02 cm^{-1} by their averaged values, respectively. Their uncertainties were estimated from the standard deviation of their eleven values in different field strength. The line width Γ_R was in good agreement with the band width of the laser light. The efficiency $\gamma(B)$ is shown in Figure 5. Its uncertainty was estimated from the deviation between $I(\nu, B)$ and $I_{Cal}(\nu, B)$ for each strength B. The resultant calculated product $\sigma_{J''M''}P(\nu, B)$ is shown in Figure 4b with the transition frequency resonated with the $X^2\Pi - A^2\Sigma^+$ transition (dashed line). In the calculation, rotational levels of $J = 0.5 - 4.5$ of the $A^2\Sigma^+$ state were included. Figure 4c shows the assignment of the $X^2\Pi_{1/2}(v'' = 0, J'' = 5.5, M'' = M \mp 1) - A^2\Sigma^+F_1(v = 0, J = 4.5, M)$ transition by the magnetic quantum numbers M, M'', for example.

From a comparison of Figures 4a with 4b, transition lines were assigned as followings. In $B = 0$ T, the succession of the M-degenerated rotational $X^2\Pi_{1/2}(v'' = 0, J+1, M \mp 1) - A^2\Sigma^+F_1(v = 0, J, M)$ transition lines (P_1-branch) was clearly observed, where the quantum number J was shown in the figure [26,28]. As the field strength B was increased, each line split into two components. This splitting was due to the Zeeman splitting of the intermediate $A^2\Sigma^+F_1(v = 0, J, M)$ sublevel into two sublevels corresponding to $\pm 1/2$ components of the electronic spin. For the larger field strength near 10 T, the width of the each component became broader. This broadening was due to the Zeeman splitting of the ground

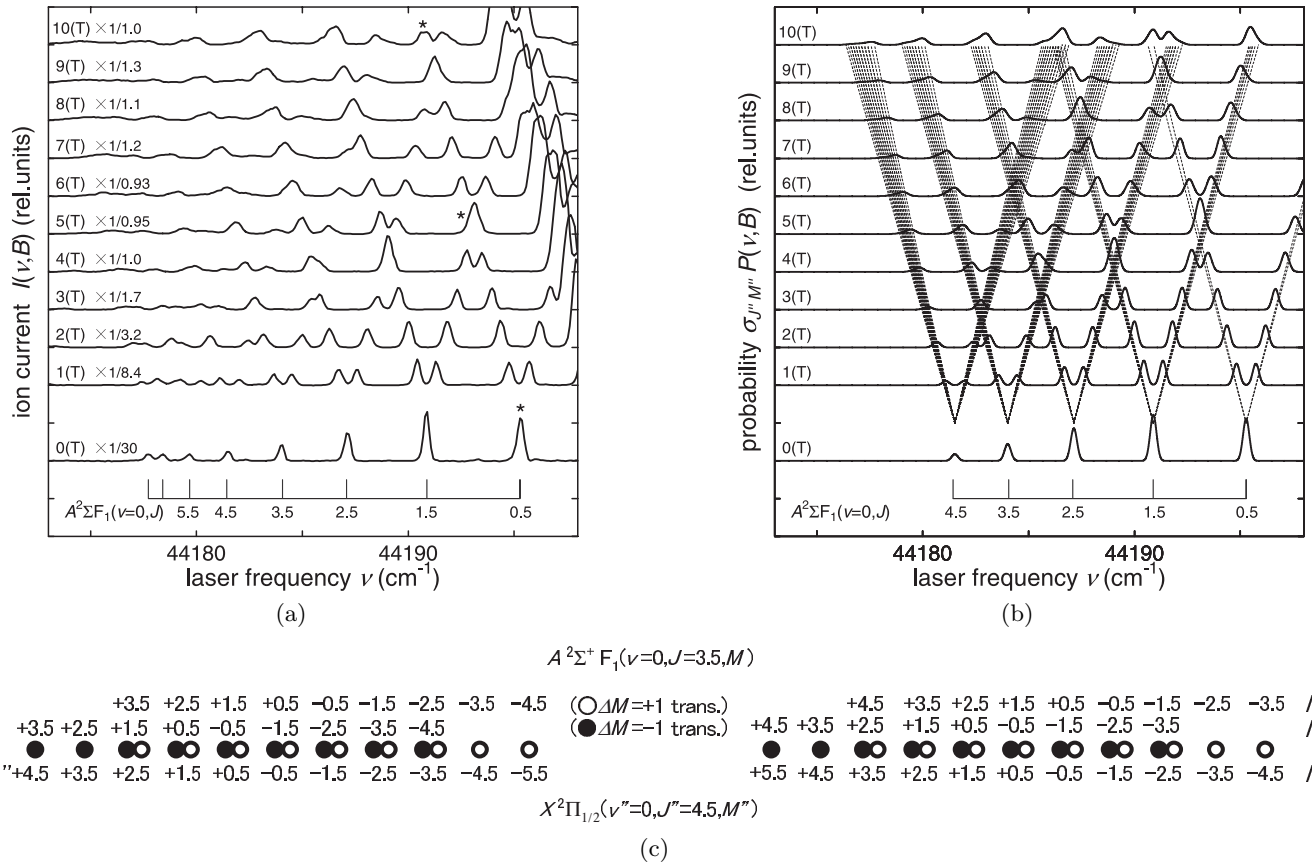

Fig. 4. (a) Observed integrated ion current $I(\nu, B)$ normalized by the laser power, due to the REMPI process through the $X^2\Pi_{1/2}(v = 0, J + 1, M \mp 1) - A^2\Sigma^+F_1(v = 0, J, M)$ transition. The abscissa is the frequency of the laser light. It is linearly polarized perpendicular to the magnetic field. The quantum number J of the intermediate $A^2\Sigma^+F_1(v = 0, J, M)$ level is shown below the transition line in a zero field. Notice that the current $I(\nu, B)$ is factored by the number written above its curve, so that the relative strength of $I(\nu, B)$ seen in the figure is equivalent to that of the calculated product $\sigma_{J''M''}P(\nu, B)$ shown in Figure 4b. Notice also that the denominators of those numbers divided by 30.0 are equivalent to $\gamma(B)$ shown in Figure 5. The asterisks denote the transition lines excited in the measurement shown in Figure 2. (b) Calculated product $\sigma_{J''M''}P(\nu, B)$ is shown by the solid curve. The dashed curve represents the calculated frequency of the $\Delta M = \pm 1$ transition. (c) The assignment of the $X^2\Pi_{1/2}(v'' = 0, J'' = 5.5, M'' = M \mp 1) - A^2\Sigma^+F_1(v = 0, J = 4.5, M)$ transition, energy of which is shown by the dashed curve in (b). The open circle represents the $\Delta M = +1$ transition and the closed one $\Delta M = -1$ transition. The magnetic quantum numbers M, M'' of the intermediate and the lower sublevels are shown. Among the 36 lines, 14 pairs of lines are degenerated in energy.

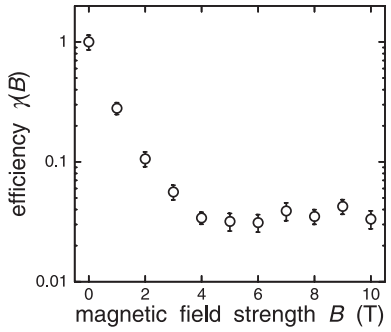

Fig. 5. Variation of the efficiency of the detection $\gamma(B)$ on the magnetic field strength B, which is normalized by $\gamma(B = 0) = 1$.

$X^2\Pi_{1/2}(v'' = 0, J+1, M \mp 1)$ sublevel [26]. It was also understood from these figures that since T_R was reflected in the relative strength between the transition lines in each field strength B, while $\gamma(B)$ was reflected in the relative strength between the same transition line observed in the different field strength B, the parameters T_R and $\gamma(B)$ were able to be determined uniquely.

Below $B = 4$ T, the efficiency $\gamma(B)$ decreased as the field strength B increased, but above $B = 4$ T, $\gamma(B)$ was almost constant of 4%. Figures 2c, 2d and Figure 4a showed that the efficiency of 4% was sufficient enough to measure the laser-frequency dependence of the ionization probability though the REMPI process with a sufficient S/N ratio. Figures 3 and 5 showed that the present arrangement of a superconducting magnet, a molecular beam source, einzel lenses, and the time-of-flight technique, would be valid for obtaining both the sufficient mass resolution and the sufficient ion current for the stronger field above 10 T.

Experimental set-up for studying the effects of the strong magnetic field on the structure and the decay

dynamics of molecules, was designed and constructed. Its performance was demonstrated using the REMPI process of NO molecules. The mass resolution $m/\Delta m \geq 180 \pm 6$ and the sufficient ion current were obtained in the field up to 10 T. This was the first successful result which demonstrating the sufficient mass resolution obtained by the time-of-flight technique in the strong magnetic field up to 10 T.

References

1. F.A. Jenkins, E. Segre, Phys. Rev. **55**, 52 (1939)
2. W.R.S. Garton, F.S. Tomkins, Astrophys. J. **158**, 839 (1969)
3. A.R. Edmonds, J. Phys. B **6**, 1603 (1973)
4. R.J. Fonck, F.L. Roesler, D.F. Tracy, K.T. Lu, F.S. Tomkins, W.R.S. Garton, Phys. Rev. Lett. **39**, 1513 (1977)
5. M.L. Zimmerman, J.C. Castro, D. Kleppner, Phys. Rev. Lett. **40**, 1083 (1978)
6. C.W. Clark, K.T. Taylor, J. Phys. B **13**, L737 (1980)
7. A.F. Starace, J. Phys. B **6**, 585 (1973)
8. R.J. Fonck, D.H. Tracy, D.C. Wright, F.S. Tomkins, Phys. Rev. Lett. **40**, 1366 (1978)
9. K.T. Lu, F.S. Tomkins, H.M. Crosswhite, H. Crosswhite, Phys. Rev. Lett. **41**, 1034 (1978)
10. K.T. Lu, F.S. Tomkins, W.R.S. Garton, Proc. R. Soc. Lond. A **362**, 421 (1978)
11. J.C. Castro, M.L. Zimmerman, R.G. Hullet, D. Kleppner, R.R. Freeman, Phys. Rev. Lett. **45**, 1780 (1980)
12. S. Nuzzo, M.R.C. McDowell, J. Phys. B **16**, 3895 (1983)
13. R.H. Garstang, Rep. Prog. Phys. **40**, 105 (1977)
14. *Progress in atomic spectoroscopy*, H.J. Beyer, H. Kleinpoppen (Plenum, 1984), Part C, Chaps. 6 and 7
15. S. Guizard, N. Shafizadeh, M. Horani, D. Gauyacq, J. Chem. Phys. **94**, 7046 (1991)
16. N. Shafizadeh, M. Raoult, M. Horani, S. Guizard, D. Gauyacq, J. Phys. II (France) **2**, 683 (1992)
17. A. Matzkin, M. Raoult, D. Gauyacq, Phys. Rev. A **68**, 061401 (2003)
18. T.S. Monteiro, K.T. Taylor, J. Phys. B **23**, 427 (1990)
19. A. Matzkin, T.S. Monteriro, Phys. Rev. Lett. **87**, 143002 (2001)
20. M. Raoult, S. Guizard, D. Gauyacq, A. Marzkin, J. Phys. B **38**, S171 (2005)
21. K. Takazawa, H. Abe, J. Chem. Phys. **110**, 11682 (1999)
22. W.M. Huo, J. Chem. Phys. **52**, 3110 (1970)
23. D. Proch, T. Trickl, Rev. Sci. Instrum. **60**, 713 (1989)
24. W.C. Wiley, I.H. McLaren, Rev. Sci. instrum. **26**, 1150 (1955)
25. W. Demtröder, *Laser Spectroscopy* (Springer, 1996)
26. K. Takazawa, H. Abe, J. Chem. Phys. **110**, 9492 (1999)
27. T. Fujimoto, *Plasma Spectroscopy* (Oxford Science Press, 2004)
28. D.W. Robinson, J. Chem. Phys. **50**, 5018 (1969)